Should Cities Embrace Their Heat Islands as Shields from Extreme Cold?

JIACHUAN YANG AND ELIE BOU-ZEID

Department of Civil and Environmental Engineering, Princeton University, Princeton, New Jersey

ABSTRACT

The higher temperature in cities relative to their rural surroundings, known as the urban heat island (UHI), is one of the most well documented and severe anthropogenic modifications of the environment. Heat islands are hazardous to residents and the sustainability of cities during summertime and heat waves; on the other hand, they provide considerable benefits in wintertime. Yet, the evolution of UHIs during cold waves has not yet been explored. In this study, ground-based observations from 12 U.S. cities and high-resolution weather simulations show that UHIs not only warm urban areas in the winter but also further intensify during cold waves by up to $1.32° \pm 0.78°C$ (mean $\pm$ standard deviation) at night relative to precedent and subsequent periods. Anthropogenic heat released from building heating is found to contribute more than 30% of the UHI intensification. UHIs thus serve as shelters against extreme-cold events and provide benefits that include mitigating cold hazard and reducing heating demand. More important, simulations indicate that standard UHI mitigation measures such as green or cool roofs reduce these cold-wave benefits to different extents. Cities, particularly in cool and cold temperate climates, should hence revisit their policies to favor (existing) mitigation approaches that are effective only during hot periods.

1. Introduction

The increasing shift in population toward cities drives the continual expansion of urban land use worldwide (Seto et al. 2012). The concomitant urban heat islands already affect more than 4 billion city residents and are intensifying along with their impacts on health, energy consumption, ecosystem services, and water and air quality (Patz et al. 2005; Grimm et al. 2008; Rizwan et al. 2008). Repercussions of these impacts extend far beyond the footprint of urban agglomerations through greenhouse gas emissions, intense resource use, and myriad modifications of the geohydrosphere (Rees and Wackernagel 1996; Satterthwaite 2008). Observed temperature increases within cities far exceeded the global warming signal in the past century (Peng et al. 2012; Pachauri et al. 2014) and will continue to grow in the foreseeable future as cities expand (Kalnay and Cai 2003; Chen et al. 2006). The emergence of megacities of historically unprecedented extent over the past few decades has made the urban heat island (UHI) quite a ''hot'' topic,

with studies documenting its extent for almost every major city (Stewart 2011). As the name ''heat island'' would suggest, a significant portion of the UHI literature has focused on summertime or heat-wave conditions (Laaidi et al. 2012; Li and Bou-Zeid 2013) in which the local urban heat anomaly exacerbates the already hot weather, the health risk for residents, and cooling demands for buildings. Cities have consequently invested substantial resources to try to mitigate the adverse impacts (Rosenzweig et al. 2006; Gartland 2012, Santamouris 2013).

During cold periods, on the other hand, heat islands could provide benefits to cities and their residents by warming the built environment. Previous studies on the urban energy balance established that for cool and cold climate zones UHI intensity in winter is larger than during other seasons (Kim and Baik 2005; Hinkel and Nelson 2007). Heat islands were found to reduce heating demand for buildings, with significant impacts on annual energy consumption for cities where energy use for heating is substantial (Sun and Augenbroe 2014). When applying knowledge of urban climate to guide the planning process, both summertime penalties and wintertime benefits of UHIs hence need to be considered (Ren et al. 2011). These wintertime benefits are expected to be significant during extremely cold periods, but studies that focus on UHI development during cold

Corresponding author: Jiachuan Yang, jiachuan@princeton.edu

TABLE 1. Location of urban and representative rural stations for the studied cities.

Cities	Urban station	Rural station	Rural land use
New York, NY	40.789°N, 73.967°W	40.876°N, 74.283°W	Pasture/hay
Chicago, IL	41.786°N, 87.752°W	41.843°N, 88.851°W	Cultivated crops
Philadelphia, PA	39.868°N, 75.231°W	40.330°N, 75.123°W	Cultivated crops
Indianapolis, IN	39.732°N, 86.279°W	39.630°N, 86.814°W	Cultivated crops
Columbus, OH	39.991°N, 82.877°W	39.840°N, 83.840°W	Cultivated crops
Detroit, MI	42.409°N, 83.010°W	41.868°N, 84.079°W	Cultivated crops
Milwaukee, WI	42.955°N, 87.904°W	42.690°N, 88.304°W	Cultivated crops
Minneapolis, MN	44.883°N, 93.229°W	44.476°N, 93.016°W	Cultivated crops
Pittsburgh, PA	40.355°N, 79.922°W	40.777°N, 79.950°W	Pasture/hay
Buffalo, NY	42.941°N, 78.736°W	42.150°N, 79.250°W	Cultivated crops
Louisville, KY	38.181°N, 85.739°W	38.095°N, 84.747°W	Pasture/hay
Des Moines, IA	41.534°N, 93.653°W	41.556°N, 93.286°W	Cultivated crops

waves remain lacking. The amenities of wintertime UHIs become exceedingly important for extreme cold during which local urban warming by even a few degrees can be vital. For example, a 1°C decrease in minimum temperature raises the daily total deaths in European cities by 1.35% during the cold season (Analitis et al. 2008). Although cold temperatures alone might not be the primary driver of high winter mortality (Ebi 2015; Kinney et al. 2015), extreme-cold events still pose a serious hazard to urban residents (Conlon et al. 2011; Berko et al. 2014). Although UHI-induced warming was found to nonlinearly aggravate heat waves in cities (Li and Bou-Zeid 2013), its interaction with cold waves remains undetermined, and hence the implications of this interaction cannot be accounted for when cities plan UHI mitigation initiatives.

It is therefore imperative to examine the evolution of UHIs during critical cold-wave periods and how this evolution is potentially altered by the implementation of mitigation measures, but such studies remain missing from the literature. This study bridges this gap by addressing the following questions. To what extent will the UHI intensify or weaken under anomalously low regional temperatures? Will commonly used mitigation measures weaken wintertime UHI and limit its potential benefits during cold waves? The findings allow us to assess the interaction between cold-wave hazards and the urban environment as well as to provide more comprehensive guidance to policy makers on the need for appropriate mitigation measures that limit summertime UHI with negligible change to the wintertime UHI.

2. Method

a. Temperature data

The early 2014 North American cold wave was selected as our study period. The extreme event was caused by a southward-moving cold air mass resulting from an atypical polar vortex, which reached as far south as Dallas, Texas, and set more than 49 record lows on 7 January across the United States. We collected hourly air temperature data at weather stations from the National Centers for Environmental Information (https://www.ncdc.noaa.gov/) and the Automated Surface Observing System (http://www.nws.noaa.gov/asos/) to derive UHI intensity [defined here as the 2-m air temperature difference between urban and rural stations (ΔT_{2m})] in this study. Cities were chosen to achieve a sufficient spatial coverage of the Northeast and Midwest regions of the United States to verify the generality of the findings across geographical conditions. In each city, we used the closest weather station to city center as the urban station. Among the weather stations completely outside the urban sprawl, we selected the representative rural station with measurements over the dominant land-use type, as based on the latest National Land Cover Database 2011 (Homer et al. 2015). Detailed information on stations for individual cities is summarized in Table 1.

b. High-resolution weather simulation

The Advanced Research version (3.5.1) of the Weather Research and Forecasting (WRF) Model, an integrated land–atmosphere framework developed by the National Center for Atmospheric Research (Skamarock and Klemp 2008), was used for high-resolution weather simulations in this study. The WRF Model is a powerful numerical tool with successful applications over major metropolitan areas around the world (Chen et al. 2011). Urban land surface is modeled as a "canyon" structure through a single-layer urban canopy model (UCM; Kusaka et al. 2001), which accounts for modified thermal properties of anthropogenic materials, anthropogenic heat release, shading, and reflection from buildings. Recent developments of the model that is used here allow

users to 1) simulate the subfacet heterogeneity of urban surfaces [e.g., the ground surface consists of concrete, asphalt, and vegetation (Wang et al. 2013)], and 2) faithfully represent hydrological processes in the urban area, including green roofs (Li et al. 2014; Yang et al. 2015). A constant-temperature boundary condition of 21°C was used at the building inner surfaces to represent indoor heating during the simulation period. This will dynamically capture the anthropogenic heat release related to space heating as it is conducted outward through the building walls and roofs and also will reproduce how this heat release increases with colder outdoor temperature.

We used a nested-domain configuration (Fig. 1a) to output high-resolution results around Chicago, Illinois, with a reasonable incorporation of large-scale meteorological forcing. We selected Chicago for the focused high-resolution numerical experiments that aim to probe the physical processes that modulate UHI evolution because of its evident UHI intensification during both daytime (Fig. 2b) and nighttime (Fig. 2c), which is later demonstrated in Fig. 2 to be representative of most studied cities. The outer (D01), middle (D02), and inner (D03) domains had resolutions of 9, 3, and 1 km, respectively. Spatial variation of land use/land cover was represented using the latest National Land Cover Database 2011 (Homer et al. 2015), as illustrated for D02 and D03 in Fig. 1b. To increase the accuracy of the land surface heterogeneity representation further, we used a mosaic approach to solve for multiple land-use categories at every WRF grid cell (Li et al. 2013), which previously had contained one single dominant category. Accurate simulation of snow in cities remains an open challenge owing to complex anthropogenic activities that cannot be well represented in weather models, but snow cover is represented realistically over all land-use types other than the urban categories. The mosaic approach mitigates the impact of incomplete urban snow-cover details, and the validation against observations that is reported later in this study indicates that this situation does not pose a significant burden on the model's performance. Data for initial and boundary conditions were obtained from the North American Regional Reanalysis from the National Centers for Environmental Prediction (https://rda.ucar.edu/datasets/ds608.0/).

We ran the simulations from 0000 UTC 22 December 2013 to 0000 UTC 13 January 2014, with an output frequency of 1 h. A 3-day period spanning 22–24 December was treated as the spinup period, and the results were analyzed only for 25 December–13 January. The spatial average of temperature over a 0.2° × 0.2° extent centered at the chosen urban and rural station was used to derive model-predicted UHI for individual cities within the simulated domain. When modeling mitigation measures,
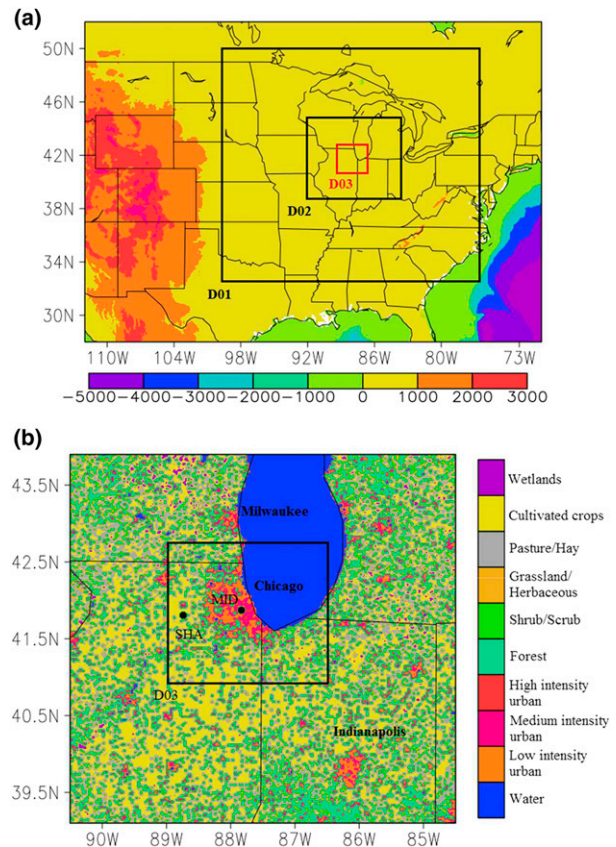

FIG. 1. High-resolution weather-simulation domains: (a) geographical representation of the domain extent with elevation (m) overlaid and (b) land-use and land-cover information around the higher-resolution domains.

"conventional roof" was replaced by "cool roof" and "green roof" across all urban grid cells. The initial soil moisture of the 0.3-m-deep soil layer of the green roof is assumed to be the same as that in the surrounding natural lands.

c. Heating degree-day

The heating degree-day (HDD) for a city during any given day is

$$\text{HDD} = T_{\text{ref}} - T_a, \qquad (1)$$

where T_{ref} is a reference temperature of 18°C and T_a is the daily average outdoor air temperature in degrees Celsius. When T_a is greater than T_{ref}, HDD is 0 for that day. In this study, we used T_{2m} in urban areas as T_a for estimation of total heating degree-days.

3. Observed intensification of UHIs during extreme cold

Reduced evapotranspiration and augmented storage of thermal energy in urban materials, relative to vegetated
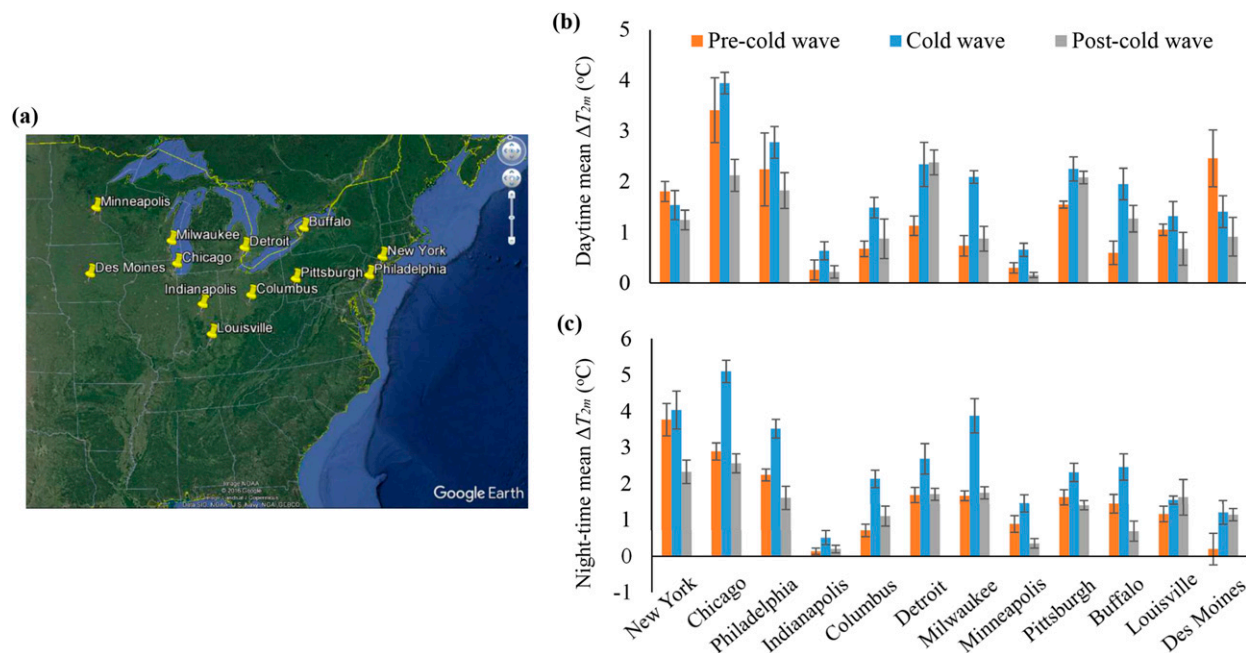
FIG. 2. (a) The locations of the 12 studied U.S. cities (courtesy of Google Earth), and their observed UHIs during the early 2014 North American cold wave: (b) daytime (0800–1600 local time) and (c) nighttime (1700–0700 local time) mean ΔT_{2m}.

rural areas, are two of the principal causes of UHIs (Oke 1982). During cold waves, however, even when vegetation is present, freezing temperatures diminish the evaporative demand of the air and reduced net radiation diminishes the available energy; this condition hinders evapotranspiration regionally and reduces the vegetation cooling differential between urban and rural areas. Anthropogenic materials also would tend to store less energy if incoming radiation is reduced because of increased cloud cover and decreased solar input. As a first guess, UHIs thus appear to weaken during cold waves.

In a surprising result, however, weather-station observations in 12 U.S. cities (Fig. 2a) show that UHIs (ΔT_{2m}) intensified during the early 2014 North American cold wave during daytime (9 of 12 studied cities; Fig. 2b) and, even more noticeable, during nighttime (11 of 12 studied cities; Fig. 2c). To avoid uncertainties from imprecise definitions of cold waves, the start and end of this cold wave were delineated, respectively, by a continuous decrease and increase in hourly 2-m air temperature T_{2m} of more than 15°C in less than 24 h (magnitude varies among cities; see, e.g., Fig. 3a). The nighttime UHI intensification during the cold wave (1.32° ± 0.78°C, mean ± standard deviation among all cities) is 2 times its daytime counterpart (0.65° ± 0.34°C). The weak relationship between UHIs and population size is partially due to the different distances between representative urban and rural stations

over the studied cities. Without invoking any physical explanation yet, it is clear that urban areas provide a higher resistance to the invading cold wave than do surrounding rural areas.

4. WRF simulation results

Findings from point-scale station measurements require validation over a wider spatial extent to confirm their applicability at the city scale. Persistent cloudy weather impairs the acquisition of remote sensing images during the cold wave, but spatial analysis of UHI through high-resolution WRF simulations offers a compelling alternative. Good agreement between predicted and observed T_{2m} (coefficient of determination $R^2 = 0.97$; root-mean-square error of 1.36°C), with the record low T_{2m} of −25°C on 6 January reproduced well, validates the skill of the model (Fig. 3a).

A closer look at the daily variation of observed UHIs in Chicago reveals that nighttime ΔT_{2m} exceeds daytime ΔT_{2m} during the cold wave (Fig. 3b). Model results reaffirm this phenomenon at the city scale (Fig. 3c) and demonstrate the capacity of heat islands to preserve effectively a warmer urban thermal environment, in particular at night. The predicted UHIs of Milwaukee, Wisconsin, and Indianapolis, Indiana, in the medium-resolution domain reinforce this finding (Fig. 4). The intensified nighttime UHIs could reduce the cold hazard by attenuating the extremely low nocturnal temperatures.
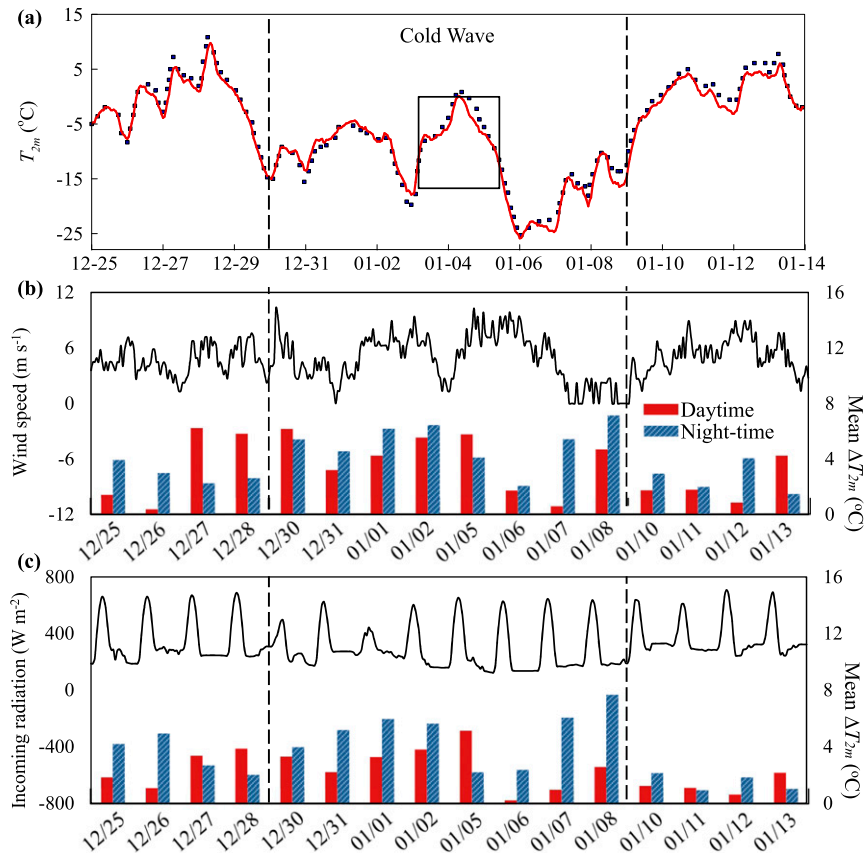
FIG. 3. Evolution of meteorological conditions and UHI in Chicago through the cold wave: (a) observed (filled squares) and predicted (red line) T_{2m} at Chicago Midway Airport, (b) mean ΔT_{2m} (bars), and wind speed (black line) from weather stations, and (c) spatially averaged mean ΔT_{2m} (bars) over a $0.2° \times 0.2°$ area centered at the weather stations, along with incoming total radiation (black line) from the model.

Furthermore, these UHI shielding benefits are also clear during daytime, as well as before and after the cold-wave period.

We now turn our attention to the development of a mechanistic understanding of how UHIs evolve during cold spells. The temporal variability of the UHI magnitude correlates weakly with weather conditions (wind speed and incoming total radiation) during this extreme event (Figs. 3b,c). The simulation data indicate that the difference in net radiation flux between urban and rural areas ΔR_n $(=R_{n,\text{urban}} - R_{n,\text{rural}})$ is a key determinant of the daytime ΔT_{2m}. Despite reduced incoming total radiation, mean daytime ΔR_n during the cold wave $(103.76 \, \text{W m}^{-2})$ is about 30% more than before or after $(79.05 \, \text{W m}^{-2}$; Fig. 5a). The increased ΔR_n can be partially attributed to the expanded gap between urban snow cover and rural snow cover, as anthropogenic activity (e.g., road cleaning or heat release) accelerated melting and reduced the presence of high-albedo snow surface in cities. Because of the augmented snow coverage

difference (Fig. 5b), rural land surface albedo becomes increasingly larger than urban land surface albedo during the cold wave (from 0.37 before the cold wave to 0.43 during the cold wave). This phenomenon is consistent with previous in situ wintertime measurements in Montreal, Quebec, Canada (Bergeron and Strachan 2012).

On the other hand, we find that the surge in nighttime ΔT_{2m} is modulated by the heat release from the urban fabric, which is the primary source for nocturnal surface energy balance. Daytime radiative flux nevertheless continues to have a significant indirect effect because it allows for the larger subsurface storage that sustains heat release at night while the remaining part of the nocturnal heat release is supplied by anthropogenic space heating. This "thermal battery" function of the urban fabric is seen not only over one diurnal cycle but over multiple days too. With regard to the impact of the cold wave on the thermal dynamics of the urban fabric, the stimulation of nighttime heat release (nighttime mean during the cold wave minus the nighttime mean of
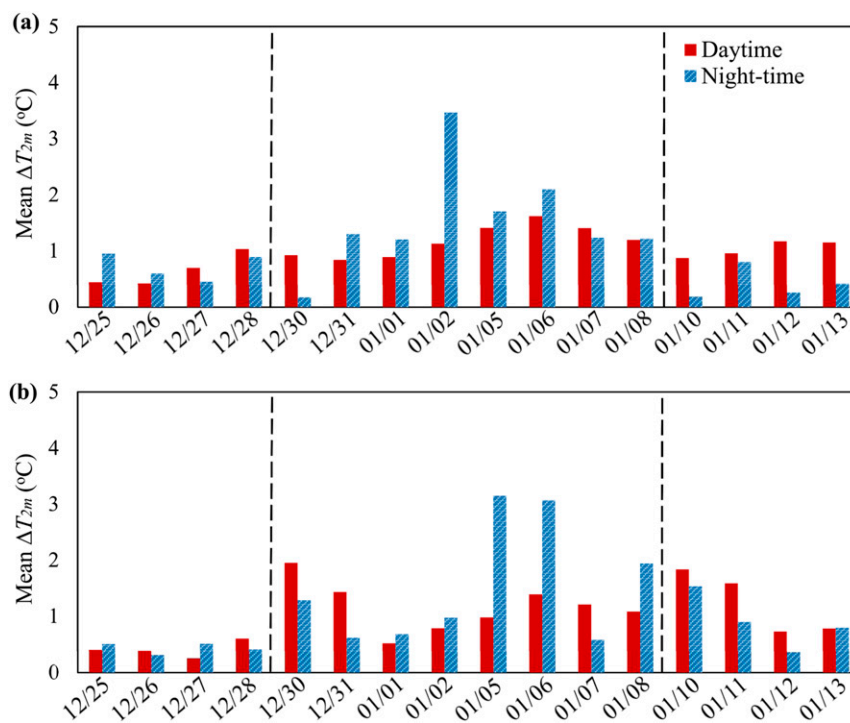
FIG. 4. Variation of model-predicted mean ΔT_{2m} in the medium-resolution domain: (a) Milwaukee and (b) Indianapolis.

pre-cold-wave periods in Fig. 6a; $-34.86\,\mathrm{W\,m^{-2}}$) far outweighs the cut in daytime energy absorption (daytime mean during the cold wave minus the daytime mean of pre-cold-wave periods in Fig. 6a; $17.05\,\mathrm{W\,m^{-2}}$). The urban fabric is thermally charged during the relatively warm pre- and post-cold-wave periods (positive daily average in Fig. 6b) and discharges (negative daily average in Fig. 6b) to supply heat for cities during the cold wave. The large thermal inertia of anthropogenic materials makes cities much better thermal capacitors than natural terrain, allowing cities to store and release substantially more energy when background temperature drops are identical. As the cold wave sets in, the mean difference in nighttime heat release between urban and rural areas grows from 18.2 to $44.7\,\mathrm{W\,m^{-2}}$ (Fig. 6a). The presence of buildings and vertical obstacles that create complex built-up topographies traps the released heat inside the urban canopy and insulates the cities against cold air masses. Similar results in Milwaukee and Indianapolis indicate that the finding is not unique to Chicago (Fig. 7).

5. Impact of anthropogenic heat

In urban areas, anthropogenic heat provides a substantial amount of additional energy into the surface energy balance. The major sources of urban anthropogenic heat include vehicles, buildings, and industry. Estimating emissions from vehicles requires spatial and temporal distributions of vehicle trips within the city and the distribution of vehicle types on roads throughout the day, which are not available at a daily basis for most metropolitan areas (Sailor 2011). Therefore, anthropogenic heat from vehicle traffic is calculated on the basis of annual summaries of vehicle data (Sailor and Lu 2004). The industrial sector has much more uniform emissions than do other sectors, and thus its energy consumption can be assumed to be constant throughout the year (Sailor 2011). On the other hand, anthropogenic heat from buildings is strongly related to the weather and can be estimated on an hourly basis from the outdoor air temperature (Sailor and Lu 2004). As explained before, the UCM dynamically captures the heat released through space heating in residential, commercial, and industrial buildings; the heat released from transportation and industrial processes needs to be added.

To distinguish the impact of this added anthropogenic heat mainly from transportation and industrial processes on the intensification of UHIs during the cold wave, we first conducted a set of three simulations with different magnitudes of added anthropogenic heat: 1) no anthropogenic heat (NoAH), 2) regular anthropogenic heat (AH), and 3) double anthropogenic heat (DblAH).
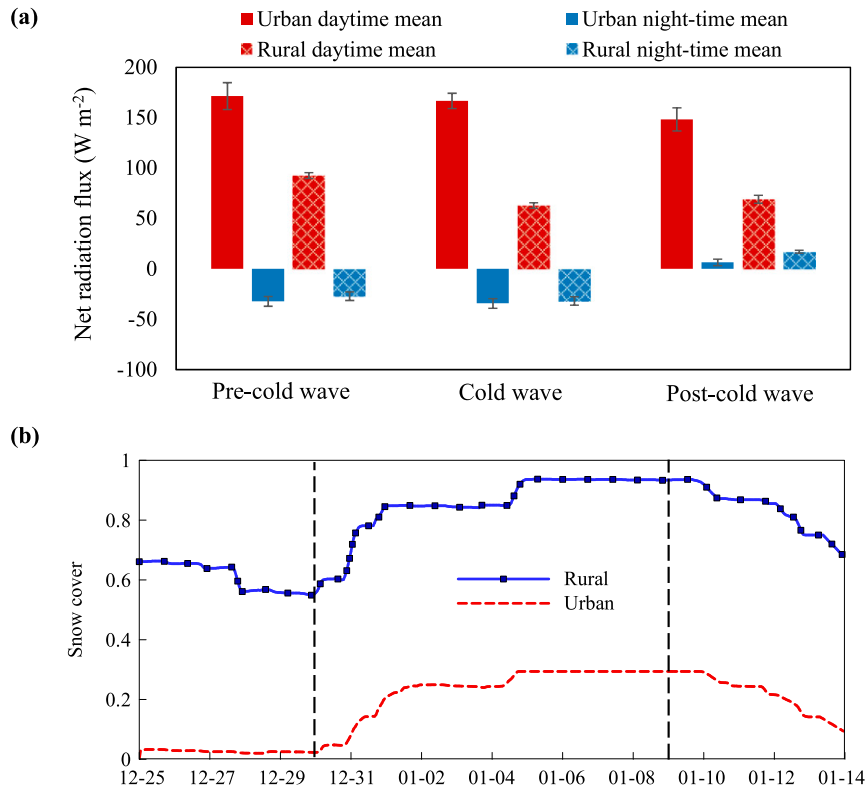
(a)

(b)

FIG. 5. Variation of model-predicted (a) mean net radiation flux and (b) snow cover in Chicago across the cold wave.

This set of simulations can quantify the impact of the uncertainty related to heat emissions from vehicle and industrial processes on the intensification of UHIs. In the regular AH scenario, anthropogenic heat is modeled as a fixed 24-h profile (no day-to-day variation) across the simulation period, with a daily peak of 60, 45, and $30 \, W \, m^{-2}$ for commercial, high-density residential, and low-density residential urban land use, respectively. Figure 8 shows that heat-island intensity increases with the magnitude of added anthropogenic heat throughout the simulation period. For each scenario, the increases in UHI caused by the mean anthropogenic heat (excluding space heating) are nearly identical during pre-cold-wave, cold-wave, and post-cold-wave periods, and therefore the intensification of UHI during the cold wave is not sensitive to the outdoor anthropogenic heat added to the simulation during both daytime and nighttime. Note that the values we used in the AH case are smaller than previous estimates for Chicago using a top-down method (Sailor and Lu 2004; Sailor et al. 2015) because our values must exclude space heating, which is directly captured by the UCM. Nevertheless, the sensitivity analysis here demonstrates that our finding of UHI intensification is independent of the background mean anthropogenic heat.

To consider the AH emissions related to space heating and how they contribute to UHI intensification during the cold wave, we compared simulation results with different boundary conditions at the building inner surfaces. We performed an additional simulation with a zero-flux boundary condition at the inner surfaces of buildings, which implies no energy exchange between building envelopes and the indoor environment and thus no energy release from these perfectly insulated buildings. The regular simulations we presented up until now account for building heating through the constant-temperature boundary condition that results in heat emissions from the buildings. Therefore, we can investigate the contribution of building heating to UHI intensification during the cold wave by comparing the simulations with these two different boundary conditions. With insulated buildings, the UHI intensification drops as expected, and the magnitude of the drop indicates that building anthropogenic heating alone contributes 32.67% of the daytime UHI intensification and 40.80% of the nighttime UHI intensification during the cold wave (Fig. 9). Without building heating, daytime and nighttime intensifications are 0.91° and 1.48°C, respectively, as compared with values of 1.35°C for daytime and 2.49°C for nighttime when the heat from
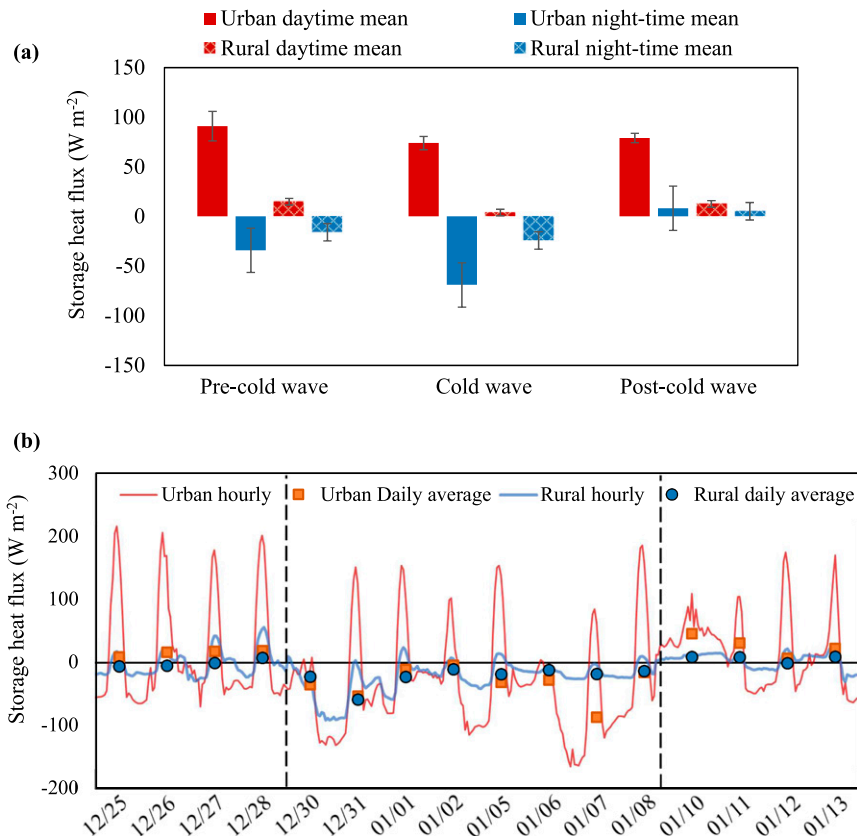
FIG. 6. Variation of model-predicted storage heat flux in Chicago across the cold wave:
(a) daytime and nighttime mean and (b) hourly and daily average.

buildings is released to the environment. These results underscore the importance of having accurate information on building insulation, which is not readily available for cities.

In terms of modeling the energy exchange between the interior of buildings and the outdoor urban environment, advanced frameworks such as a coupled multilayer urban canopy model (Martilli et al. 2002) with a building energy model (BEM; Salamanca et al. 2010) can be more accurate than the single-layer UCM used here since they additionally account for 1) radiation exchange through windows, 2) heat generation by occupants and equipment, and 3) air conditioning and ventilation heat release (in addition to heating). To take full advantage of the coupled model, however, high-resolution data of urban-canopy parameters such as canyon geometry and building characteristics are required (Chen et al. 2011). Such advanced models are more appropriate for studying the fine-resolution spatial variation within cities as well as building energy consumption. Nevertheless, the single-layer urban canopy model used in this study is sufficient for urban climate investigations at 1-km scales with moderate requirements

of input data. In addition, a single-layer UCM coupled to a mosaic land model is very useful in highly heterogeneous urban terrain, as demonstrated for New York City, New York (Ramamurthy et al. 2017), and Washington, D.C. (Li et al. 2013). Such coupling has not been tested for the BEM–building-effect-parameterization framework.

6. Implications to heat-island mitigation and urban policy

Given the demonstrated benefits of UHIs in this study, a natural question to ask is whether advancing UHI mitigation for relieving summer heat would exacerbate extreme cold. Green roofs and cool roofs are two popular measures that have been proven to be effective strategies to counteract UHIs (Sun et al. 2014; Yang and Wang 2014, 2017). The former cools the surface through evapotranspiration, and the latter reduces the temperature by reflecting incoming solar radiation. Such measures targeting UHI mitigation are mostly assessed in hot conditions, and their repercussions during cold seasons are rarely investigated excepted in a few studies (Georgescu et al. 2014). To address this question we
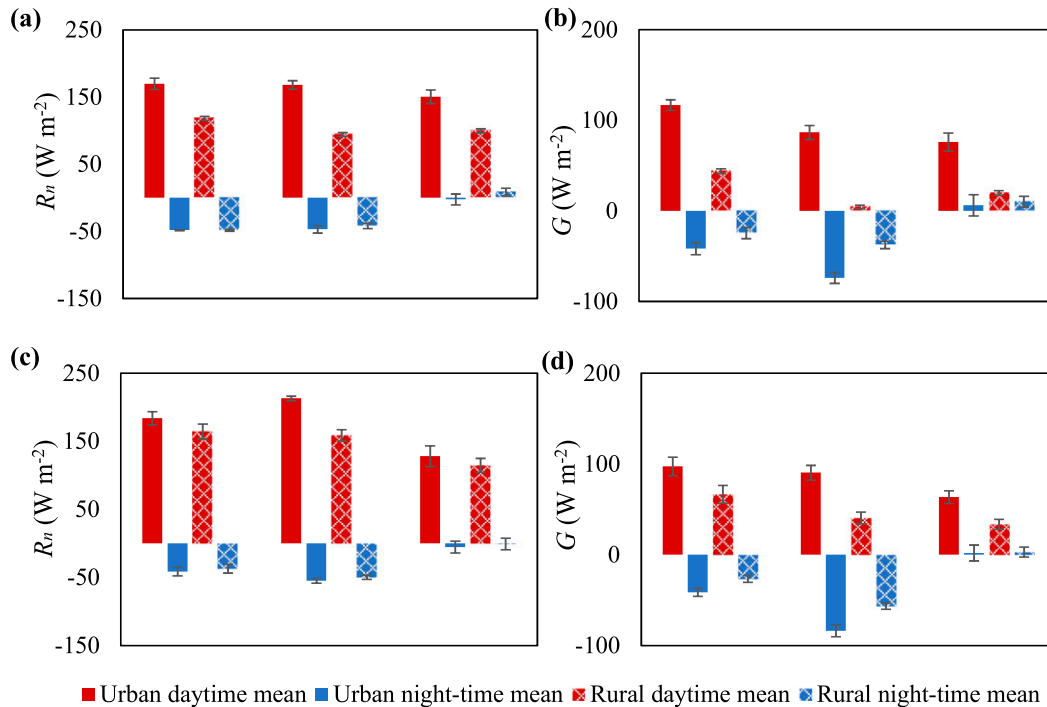
FIG. 7. Variation of model-predicted surface heat fluxes across the cold wave: mean (left) R_n and (right) G in (a),(b) Milwaukee and (c),(d) Indianapolis.

conducted the same simulation as before (with regular heat transfer in building envelope and regular AH) but converted the roofs of all built-up areas to either cool roofs or green roofs. The thermal properties of different roofs are as follows: green roofs (short grasses with loam soil; Yang et al. 2016) have an albedo of 0.23 and a thermal inertia of $1049\,J\,m^{-2}\,K^{-1}\,s^{-1/2}$, cool roofs have an albedo of 0.7 and a thermal inertia of $1442\,J\,m^{-2}\,K^{-1}\,s^{-1/2}$, and conventional roofs have an albedo of 0.17 and a thermal inertia of $1442\,J\,m^{-2}\,K^{-1}\,s^{-1/2}$.

Cool roofs reduce daytime urban T_{2m} during the cold wave by $1.38° \pm 0.08°C$ (mean $\pm$ standard deviation) but have a negligible impact on the nighttime T_{2m} (high-albedo materials are consequential only during the daytime when they reflect incoming shortwave radiation; Ramamurthy et al. 2015a,b), suggesting that they did not drastically reduce daytime thermal storage during the cold wave. Green roofs on the other hand increase daytime T_{2m} by $0.35° \pm 0.19°C$ but reduce nighttime T_{2m} by $0.51° \pm 0.14°C$ during the cold wave (Fig. 10). Low soil temperature and moisture suppress evapotranspiration severely in extreme cold (mean daytime latent heat flux increases by $4.3\,W\,m^{-2}$ with green roofs at the city scale), and hence this does not explain the impact of these roofs. The low thermal inertia of green-roof soil matrices, however, promotes the shift of energy dissipation toward atmosphere during the day (explaining the higher

daytime UHI) and reduces heat storage in the subsurface (explaining the lower nighttime UHI). Both measures are therefore not favorable during cold periods since they diminish UHI ability to act as a shelter. Green roofs could also increase building insulation and reduce heating demand and heat release to the outdoors, but the increase in daytime temperatures they produce suggests that this is not a leading physical mechanism for their influence.

Urban heat islands have important energy implications because average heating degree-days are more than 3 and 15 times the average cooling degree-days over the United States and Europe (U.S. Energy Information Administration 2012; Spinoni et al. 2015), respectively. A complete reversal of UHIs would have 1) significantly boosted the heating degree-days in Chicago [from 907 to 1030, using Eq. (1)] and New York (from 775 to 826) during the study period, 2) increased the heating energy demand and associated carbon emissions, and 3) exacerbated the low-temperature hazard posed to pedestrians and to households in fuel poverty (Marmot and Bell 2012).

7. Discussion and conclusions

The purpose of this study is to highlight the often-overlooked benefits of UHIs during extreme-cold
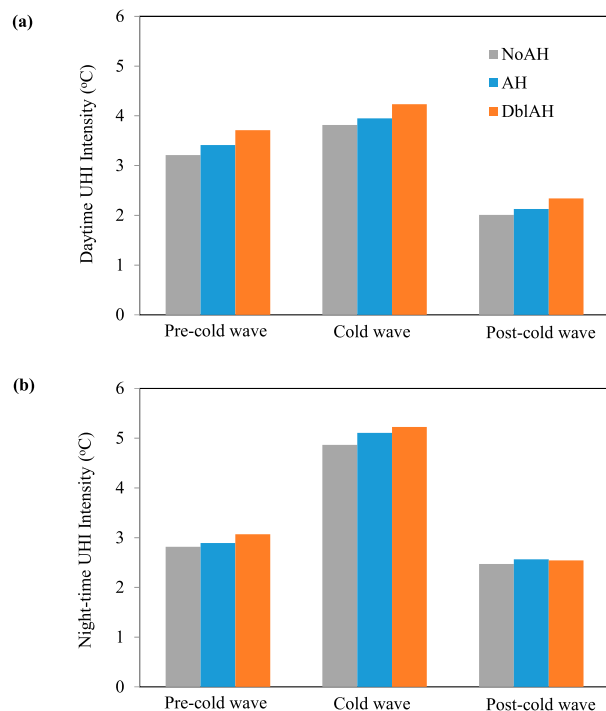
FIG. 8. Model-simulated mean (a) daytime and (b) nighttime UHI intensity across the study period with different anthropogenic heat.

FIG. 9. Contribution from building heating and other factors to the heat-island intensification during the cold wave.

spells. The findings indicate that the UHI intensifies during these extreme-cold periods, in particular during nighttime. The physical processes that explain this intensification are 1) the lower snow cover in urban areas as a result of anthropogenic snow removal, 2) the thermal-battery function of the urban fabric that stores heat during warmer periods and releases it during cold waves, and 3) building heat release from anthropogenic space heating. UHI risk under heat waves, especially with a warming climate, must remain an urgent concern for cities worldwide, but this need not overwhelm the
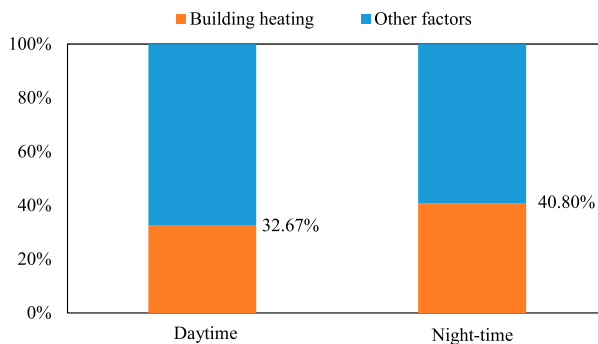
discussion of the advantages of UHIs in wintertime and in particular during extreme-cold events. This study showed that the cold-wave thermal dynamics are complex and that measures such as cool or green roofs, which usually have comparable summertime benefits, result in very distinct disbenefits during extreme-cold events. As metropoles like New York and Chicago rapidly pursue solutions for UHIs as detailed in their climate action plans (New York City Department of Environmental Protection 2008; Coffee et al. 2010), a paradigm shift is urgently needed to give an equal weight to the benefits of UHIs during wintertime and cold waves in the sustainability and resilience blueprints of cities.

To end on an optimistic note, we point out that the challenge of balancing summertime and wintertime performances and maximizing them simultaneously is not at all insurmountable, but it does require deliberate actions. Roof covers with albedos that vary with sun angle or with temperature (e.g., thermochromic materials), or other solutions that generate lower albedos in wintertime, are available (Santamouris et al. 2011; Rosso et al. 2017). In a similar way, green roofs with a
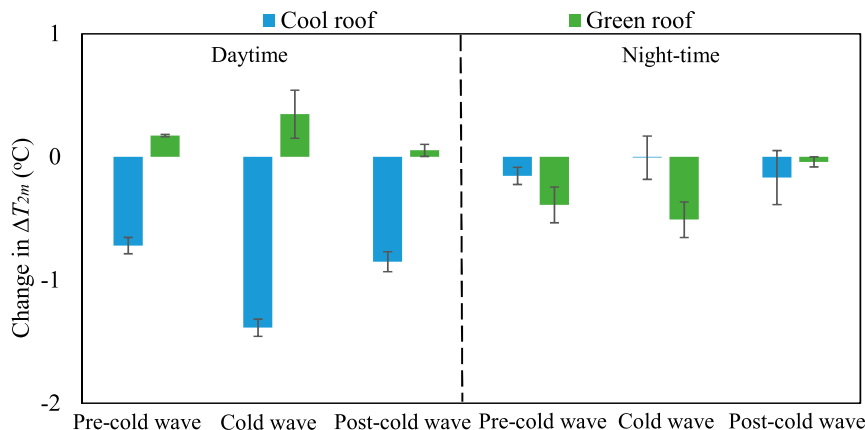

FIG. 10. Model-predicted effect of cool and green roofs on urban T_{2m}.

larger soil thermal inertia (e.g., with embedded phase-change materials) would continue to ameliorate daytime UHI conditions as shown here but would not have the same nighttime disbenefits as the widely used low-density soil roofs that were modeled in our study.

REFERENCES

Analitis, A., and Coauthors, 2008: Effects of cold weather on mortality: Results from 15 European cities within the PHEWE project. *Amer. J. Epidemiol.*, **168**, 1397–1408, https://doi.org/10.1093/aje/kwn266.

Bergeron, O., and I. B. Strachan, 2012: Wintertime radiation and energy budget along an urbanization gradient in Montreal, Canada. *Int. J. Climatol.*, **32**, 137–152, https://doi.org/10.1002/joc.2246.

Berko, J., D. D. Ingram, S. Saha, and J. D. Parker, 2014: Deaths attributed to heat, cold, and other weather events in the United States, 2006–2010. National Health Statistics Rep. 76, 16 pp., https://www.cdc.gov/nchs/data/nhsr/nhsr076.pdf.

Chen, F., and Coauthors, 2011: The integrated WRF/urban modelling system: Development, evaluation, and applications to urban environmental problems. *Int. J. Climatol.*, **31**, 273–288, https://doi.org/10.1002/joc.2158.

Chen, X. L., H. M. Zhao, P. X. Li, and Z. Y. Yin, 2006: Remote sensing image-based analysis of the relationship between urban heat island and land use/cover changes. *Remote Sens. Environ.*, **104**, 133–146, https://doi.org/10.1016/j.rse.2005.11.016.

Coffee, J. E., J. Parzen, M. Wagstaff, and R. S. Lewis, 2010: Preparing for a changing climate: The Chicago climate action plan's adaptation strategy. *J. Great Lakes Res.*, **36**, 115–117, https://doi.org/10.1016/j.jglr.2009.11.011.

Conlon, K. C., N. B. Rajkovich, J. L. White-Newsome, L. Larsen, and M. S. O'Neill, 2011: Preventing cold-related morbidity and mortality in a changing climate. *Maturitas*, **69**, 197–202, https://doi.org/10.1016/j.maturitas.2011.04.004.

Ebi, K. L., 2015: Greater understanding is needed of whether warmer and shorter winters associated with climate change could reduce winter mortality. *Environ. Res. Lett.*, **10**, 111002, https://doi.org/10.1088/1748-9326/10/11/111002.

Gartland, L. M., 2012: *Heat Islands: Understanding and Mitigating Heat in Urban Areas.* Routledge Press, 199 pp.

Georgescu, M., P. E. Morefield, B. G. Bierwagen, and C. P. Weaver, 2014: Urban adaptation can roll back warming of emerging megapolitan regions. *Proc. Natl. Acad. Sci. USA*, **111**, 2909–2914, https://doi.org/10.1073/pnas.1322280111.

Grimm, N. B., S. H. Faeth, N. E. Golubiewski, C. L. Redman, J. Wu, X. Bai, and J. M. Briggs, 2008: Global change and the ecology of cities. *Science*, **319**, 756–760, https://doi.org/10.1126/science.1150195.

Hinkel, K. M., and F. E. Nelson, 2007: Anthropogenic heat island at Barrow, Alaska, during winter: 2001–2005. *J. Geophys. Res.*, **112**, D007837, https://doi.org/10.1029/2006JF000584.

Homer, C. G., and Coauthors, 2015: Completion of the 2011 National Land Cover Database for the conterminous United States—Representing a decade of land cover change information. *Photogramm. Eng. Remote Sens.*, **81**, 345–354.

Kalnay, E., and M. Cai, 2003: Impact of urbanization and land-use change on climate. *Nature*, **423**, 528–531, https://doi.org/10.1038/nature01675.

Kim, Y. H., and J. J. Baik, 2005: Spatial and temporal structure of the urban heat island in Seoul. *J. Appl. Meteor.*, **44**, 591–605, https://doi.org/10.1175/JAM2226.1.

Kinney, P. L., J. Schwartz, M. Pascal, E. Petkova, A. Le Tertre, S. Medina, and R. Vautard, 2015: Winter season mortality: Will climate warming bring benefits? *Environ. Res. Lett.*, **10**, 064016, https://doi.org/10.1088/1748-9326/10/6/064016.

Kusaka, H., H. Kondo, Y. Kikegawa, and F. Kimura, 2001: A simple single-layer urban canopy model for atmospheric models: Comparison with multi-layer and slab models. *Bound.-Layer Meteor.*, **101**, 329–358, https://doi.org/10.1023/A:1019207923078.

Laaidi, K., A. Zeghnoun, B. Dousset, P. Bretin, S. Vandentorren, E. Giraudet, and P. Beaudeau, 2012: The impact of heat islands on mortality in Paris during the August 2003 heat wave. *Environ. Health Perspect.*, **120**, 254–259, https://doi.org/10.1289/ehp.1103532.

Li, D., and E. Bou-Zeid, 2013: Synergistic interactions between urban heat islands and heat waves: The impact in cities is larger than the sum of its parts. *J. Appl. Meteor. Climatol.*, **52**, 2051–2064, https://doi.org/10.1175/JAMC-D-13-02.1.

——, E. Bou-Zeid, M. Barlage, F. Chen, and J. A. Smith, 2013: Development and evaluation of a mosaic approach in the WRF-Noah framework. *J. Geophys. Res. Atmos.*, **118**, 918–935, https://doi.org/10.1002/2013JD020657.

——, E. Bou-Zeid, and M. Oppenheimer, 2014: The effectiveness of cool and green roofs as urban heat island mitigation strategies. *Environ. Res. Lett.*, **9**, 055002, https://doi.org/10.1088/1748-9326/9/5/055002.

Marmot, M., and R. Bell, 2012: Fair society, healthy lives. *Public Health*, **126** (Suppl. 1), S4–S10, https://doi.org/10.1016/j.puhe.2012.05.014.

Martilli, A., A. Clappier, and M. W. Rotach, 2002: An urban surface exchange parameterisation for mesoscale models. *Bound.-Layer Meteor.*, **104**, 261–304, https://doi.org/10.1023/A:1016099921195.

New York City Department of Environmental Protection, 2008: Assessment and action plan. DEP Climate Change Program Rep. 1, 102 pp., http://www.nyc.gov/html/dep/pdf/climate/climate_complete.pdf.

Oke, T. R., 1982: The energetic basis of the urban heat island. *Quart. J. Roy. Meteor. Soc.*, **108**, 1–24, https://doi.org/10.1002/qj.49710845502.

Pachauri, R. K., and Coauthors, 2014: *Climate Change 2014: Synthesis Report.* Intergovernmental Panel on Climate Change, 151 pp., http://www.ipcc.ch/pdf/assessment-report/ar5/syr/SYR_AR5_FINAL_full_wcover.pdf.

Patz, J. A., D. Campbell-Lendrum, T. Holloway, and J. A. Foley, 2005: Impact of regional climate change on human health. *Nature*, **438**, 310–317, https://doi.org/10.1038/nature04188.

Peng, S., and Coauthors, 2012: Surface urban heat island across 419 global big cities. *Environ. Sci. Technol.*, **46**, 696–703, https://doi.org/10.1021/es2030438.

Ramamurthy, P., T. Sun, K. Rule, and E. Bou-Zeid, 2015a: The joint influence of albedo and insulation on roof performance: An observational study. *Energy Build.*, **93**, 249–258, https://doi.org/10.1016/j.enbuild.2015.02.040.

——, ——, ——, and ——, 2015b: The joint influence of albedo and insulation on roof performance: A modeling study. *Energy Build.*, **102**, 317–327, https://doi.org/10.1016/j.enbuild.2015.06.005.

——, D. Li, and E. Bou-Zeid, 2017: High-resolution simulation of heatwave events in New York City. *Theor. Appl. Climatol.*, **128**, 89–102, https://doi.org/10.1007/s00704-015-1703-8.

Rees, W., and M. Wackernagel, 1996: Urban ecological footprints: Why cities cannot be sustainable—And why they are a key to sustainability. *Environ. Impact Assess. Rev.*, **16**, 223–248, https://doi.org/10.1016/S0195-9255(96)00022-4.

Ren, C., E. Y. Y. Ng, and L. Katzschner, 2011: Urban climatic map studies: A review. *Int. J. Climatol.*, **31**, 2213–2233, https://doi.org/10.1002/joc.2237.

Rizwan, A. M., L. Y. Dennis, and L. I. U. Chunho, 2008: A review on the generation, determination and mitigation of urban heat island. *J. Environ. Sci.*, **20**, 120–128, https://doi.org/10.1016/S1001-0742(08)60019-4.

Rosenzweig, C., W. Solecki, and R. Slosberg, 2006: Mitigating New York City's heat island with urban forestry, living roofs, and light surfaces. New York State Energy Research and Development Authority Final Rep. 06-06, 133 pp., https://www.nyserda.ny.gov/-/media/Files/Publications/Research/Environmental/EMEP/NYC-Heat-Island-Mitigation.pdf.

Rosso, F., A. L. Pisello, V. L. Castaldo, C. Fabiani, F. Cotana, M. Ferrero, and W. Jin, 2017: New cool concrete for building envelopes and urban paving: Optics-energy and thermal assessment in dynamic conditions. *Energy Build.*, **151**, 381–392, https://doi.org/10.1016/j.enbuild.2017.06.051.

Sailor, D. J., 2011: A review of methods for estimating anthropogenic heat and moisture emissions in the urban environment. *Int. J. Climatol.*, **31**, 189–199, https://doi.org/10.1002/joc.2106.

——, and L. Lu, 2004: A top-down methodology for developing diurnal and seasonal anthropogenic heating profiles for urban areas. *Atmos. Environ.*, **38**, 2737–2748, https://doi.org/10.1016/j.atmosenv.2004.01.034.

——, M. Georgescu, J. M. Milne, and M. A. Hart, 2015: Development of a national anthropogenic heating database with an extrapolation for international cities. *Atmos. Environ.*, **118**, 7–18, https://doi.org/10.1016/j.atmosenv.2015.07.016.

Salamanca, F., A. Krpo, A. Martilli, and A. Clappier, 2010: A new building energy model coupled with an urban canopy parameterization for urban climate simulations—Part I. Formulation, verification, and sensitivity analysis of the model. *Theor. Appl. Climatol.*, **99**, 331–344, https://doi.org/10.1007/s00704-009-0142-9.

Santamouris, M., 2013: Using cool pavements as a mitigation strategy to fight urban heat island—A review of the actual developments. *Renewable Sustainable Energy Rev.*, **26**, 224–240, https://doi.org/10.1016/j.rser.2013.05.047.

——, A. Synnefa, and T. Karlessi, 2011: Using advanced cool materials in the urban built environment to mitigate heat islands and improve thermal comfort conditions. *Sol. Energy*, **85**, 3085–3102, https://doi.org/10.1016/j.solener.2010.12.023.

Satterthwaite, D., 2008: Cities' contribution to global warming: notes on the allocation of greenhouse gas emissions. *Environ. Urban.*, **20**, 539–549, https://doi.org/10.1177/0956247808096127.

Seto, K. C., B. Güneralp, and L. R. Hutyra, 2012: Global forecasts of urban expansion to 2030 and direct impacts on biodiversity and carbon pools. *Proc. Natl. Acad. Sci. USA*, **109**, 16 083–16 088, https://doi.org/10.1073/pnas.1211658109.

Skamarock, W. C., and J. B. Klemp, 2008: A time-split non-hydrostatic atmospheric model for weather research and forecasting applications. *J. Comput. Phys.*, **227**, 3465–3485, https://doi.org/10.1016/j.jcp.2007.01.037.

Spinoni, J., J. Vogt, and P. Barbosa, 2015: European degree-day climatologies and trends for the period 1951–2011. *Int. J. Climatol.*, **35**, 25–36, https://doi.org/10.1002/joc.3959.

Stewart, I. D., 2011: A systematic review and scientific critique of methodology in modern urban heat island literature. *Int. J. Climatol.*, **31**, 200–217, https://doi.org/10.1002/joc.2141.

Sun, T., E. Bou-Zeid, and G. H. Ni, 2014: To irrigate or not to irrigate: Analysis of green roof performance via a vertically-resolved hygrothermal model. *Build. Environ.*, **73**, 127–137, https://doi.org/10.1016/j.buildenv.2013.12.004.

Sun, Y., and G. Augenbroe, 2014: Urban heat island effect on energy application studies of office buildings. *Energy Build.*, **77**, 171–179, https://doi.org/10.1016/j.enbuild.2014.03.055.

U.S. Energy Information Administration, 2012: Annual energy review 2011. U.S. Dept. of Energy Rep. DOE/EIA-0384(2011), 370 pp., https://www.eia.gov/totalenergy/data/annual/pdf/aer.pdf.

Wang, Z.-H., E. Bou-Zeid, and J. A. Smith, 2013: A coupled energy transport and hydrological model for urban canopies evaluated using a wireless sensor network. *Quart. J. Roy. Meteor. Soc.*, **139**, 1643–1657, https://doi.org/10.1002/qj.2032.

Yang, J., and Z. H. Wang, 2014: Physical parameterization and sensitivity of urban hydrological models: Application to green roof systems. *Build. Environ.*, **75**, 250–263, https://doi.org/10.1016/j.buildenv.2014.02.006.

——, and ——, 2017: Planning for a sustainable desert city: The potential water buffering capacity of urban green infrastructure. *Landscape Urban Plann.*, **167**, 339–347, https://doi.org/10.1016/j.landurbplan.2017.07.014.

——, ——, F. Chen, S. Miao, M. Tewari, J. A. Voogt, and S. Myint, 2015: Enhancing hydrologic modelling in the coupled Weather Research and Forecasting–urban modelling system. *Bound.-Layer Meteor.*, **155**, 87–109, https://doi.org/10.1007/s10546-014-9991-6.

——, ——, M. Georgescu, F. Chen, and M. Tewari, 2016: Assessing the impact of enhanced hydrological processes on urban hydrometeorology with application to two cities in contrasting climates. *J. Hydrometeor.*, **17**, 1031–1047, https://doi.org/10.1175/JHM-D-15-0112.1.